Preparation and Application of Nano-structured Lead Dioxide from Waste Lead Slag

Xi Wang[1], *Dandan* Wu[1,2], *Du* Yuan[1], and *Xu* Wu[1,*]

[1]School of Environmental Science and Engineering, Huazhong University of Science and Technology, Wuhan, 430074, China
[2]Hubei HuaDeLai (HDL) Co. Ltd, Wuhan, 430079, China

Abstract. To develop an efficient and green method to recycling lead slag, a novel strategy to fabricate nano-lead dioxide from lead slag was applied by the hydro-electrometallurgy. In leaching system, the optimum condition of leaching time 100 min, 80 °C, stirring rate 500 rpm, liquid/solid ratio 20 and 1 mol/L methanesulfonic acid resulted in lead recovery of 89% and residue obtained without toxicity. The kinetic study revealed that the methanesulfonic acid leaching of lead slag shows good agreement with a diffusion-controlled shrinking-particle model. Additionally, the apparent activation energy of MSA leaching of lead slag was determined using Arrhenius model as 13.621 kJ/mol. Furthermore, Nano-PbO_2 recovered from waste lead paste was prepared for the electrolysis of water to produce ozone. The experimental results showed that the ozone production of nano-PbO_2 recovered from waste lead slag was not significantly different from the nano-PbO_2 prepared by pure reagents. In conclusion, waste lead slag can be recycled for the fabrication of nano-PbO_2, which has a significant advantage on realizing the recycling of lead resources.

1 Introduction

As the major solid waste generated during the smelting process of primary and secondary lead, lead slag has gained extensive focus in the environmental engineering field due to its enormous amount and high migratory toxic elements containing. Nowadays, lead slag is mainly disposed by landfill and stockpiling, which occupies extensive area [1]. However, there is a potential risk of severe pollution of surrounding environment and critical waste of resources. The high concentrations of precious metal in lead slag reconciled with the uncertain environmental stability inducing further research relating to the efficient recovery of metal lead from lead slags. Thus, growing attention has been drawn to recovery of lead slags.

Various methods for recovery of metals and decrease of the lead dispersion from lead slag are proposed. The current recycling process of lead slag includes mainly pyrometallurgical smelting, hydrometallurgical leaching and bioleaching technology [2-4]. The traditional pyrometallurgical smelting method is a widely adopted to recovering the secondary lead. But there are higher requirements for equipment and SO_2 emission and lead dust in pyrometallurgical technology can cause a hazardous threat to the environment. For this reason, many researchers draw attention to the recovery of lead via hydrometallurgy technology [5, 6]. Hydrometallurgical technology can separate and extract valuable elements from lead slag effectively and selectively. Forte [7] reported the lead recovery from lead slag via acid leaching, and this method is applicable to the recovery of metallic lead from lead residue. Nitrate-based leaching systems include HNO_3, H_2O_2-HNO_3 and Fe-HNO_3 etc. Kim [8] proposed an 2nd leaching step using HNO_3-Fe(III), about 90% of lead was leaching. However, the waste acid, waste salt, the residue and other by-products would be generated in the nitrate-based leaching systems.

As a strong organic acid, methanesulfonic acid (MSA) has many properties such as good stability, high conductivity, low toxicity, biodegradability and high solubility of metallic salts [9]. It is a polar molecule with a strong complexing ability to Pb^{2+}. In recent years, methanesulfonic acid has been used widely in Sn, Pb and Cu plating as electrolyte methanesulfonic acid leaching. In the meanwhile, methanesulfonic acid has a broad application in recovering precious metals such as Pb, Zn, Cu and Sn as lixiviant. methanesulfonic acid was a common leaching reagent to recover Pb from cerussite, galena, brass, etc. [10-11]. Therefore, methanesulfonic acid was selected and studied in the experiments.

PbO_2, as an excellent electrode material, is widely used in wastewater treatment, electrochemical measurement, and electrochemical ozone production (EOP) [12]. According to the research of Chen [13], nano-PbO_2 can improve the current efficiency of ozone production effectively, thereby reducing energy consumption. Nano-structured PbO_2 has a larger specific surface area, which increases the specific surface area of electrocatalytic activity. To realize the recycling of lead

* Corresponding author: profxuwu@hust.edu.cn.

resources, the fabrication of nano-structured lead dioxide from lead slag is proposed.

2 Materials and methods

2.1 Preparation and materials

The spent lead slag sample was collected from traditional furnaces at a lead smelting factory in Hubei Xiangyang, China. The sample was dried at 120 °C for 24 h under vacuum after crushing. Then the sample was put into a planetary high-energy ball-milling device (XQM-4) with the sealed zirconia ball-milling pot until 300 mesh.

2.2 Stability evaluation

The short-term stability of solid samples obtained from the spent lead slag and samples after leaching was assessed by the Toxicity Characteristic Leaching Procedure (TCLP), using an extraction fluid of pH 4.93±0.05. The 1000 mL extractant was made up of 5.7 mL of CH_3CH_2COOH and 64.3 mL of 1 M NaOH and deionized water. The solid samples and extractant were added to 10 mL centrifuge tubes in the solid-to-liquid ratio of 1:20, and continuously oscillated at 200 rpm for 18 ± 2 hours in a tumble shaker. Suspensions were finally filtered using 0.22 μm membrane filters.

2.3 Leaching experimental procedure

All leaching experiments of lead slag were initiated in a 200 mL beaker, which was fixed with a mechanical stirrer. First, the lead slag was added to a mixed solution of H_2SO_4 and H_2O_2, which converted lead element into lead sulphate. Then the lead sulphate was transformed into lead carbonate by ammonium carbonate. Leaching agent, methanesulfonic acid, with a desired concentration was put into the beaker and heated to a predetermined temperature before the lead carbonate was added to the beaker with agitation. After the target temperature was reached, sieved lead slag concentrate sample was added to the system.

2.4 Diaphragm electrolysis

The main part of the electrolytic cell was made of organic glass (polymethylmethacrylate, PMMA) A 2.0 cm×2.0 cm hollow was set in the opposite direction of the cathode chamber and the anode chamber (3.0 cm×4.0 cm×4.0 cm). The exchange membranes were permeated in 1 $mol \cdot L^{-1}$ NaCl solution for 12 hours and then cut into a size of 3.0 cm×3.0 cm. Then the two sides were fixed with fluorine rubber pads, the anode and cathode chamber and ion exchange membrane were pressed together with bolts assembly. The cathode and anode plates were respectively fixed by the electrode plate holders, which were made by 3D printing technology. There were slits in the middle to ensure that the electrode plates were always upright. The electrode plate holders can slide on the tank and the distance between the cathode and anode plates can be adjusted freely between 2.0 cm and 10.0 cm.

An HMTECH-A4080DT ion exchange membrane (Hangzhou Huamo Technology Co. Ltd., China) was used to separate an electrolysis cell. The ion exchange membrane was mainly synthesized from polyvinylidene fluoride, polyacrylonitrile and styrene. The important parameters for the ion of < 2.7 $\Omega \cdot cm^2$, and exchange capacity of 2.2 meq/mg. The anode plate is a fluorine-doped tin oxide (FTO) conductive glasses, and the cathode is a titanium electrode of 2.8 cm×5.0 cm. The width of the anode plate is slightly smaller than the width of the anode chamber to ensure that there is no obstruction for convection of electrolyte.

2.5 Characterization and analyzation

After all leaching experiment, the obtained filtrate was analysed by inductively coupled plasma atomic emission spectroscopy (ICP-AES, Thermo Elemental) to determine the amount of metal extraction. The original sample and obtained solid residues were analysed by X-ray diffraction (XRD, Philips) in order to determine the mineralogical composition. Scanning electron microscopy (SEM, JSM-IT300LA) was employed to characterize the morphology of precipitations.

3 Results and discussion

3.1 Characterization of lead slag

In the process of pre-treatment of the lead slag, the sample was ground into 300 mesh particles with a ball mill, and then pass them through a sieve. X-ray diffraction analysis (XRD) analysis was used for mineralogy of the slag sample with a particle size of less than 74 μm. In Fig.1, the main mineral of the Pb sample was $Pb_4(SO_4)(CO_3)_2(OH)_2$, $PbCO_3$ and SiO_2.

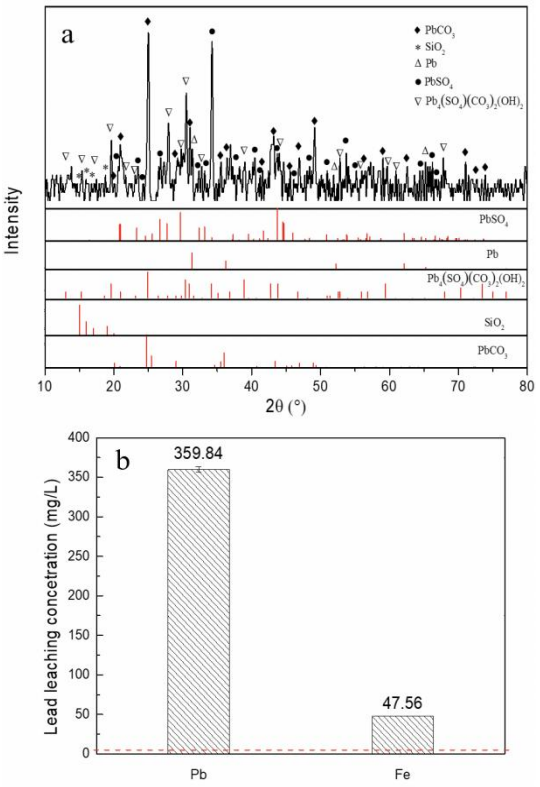

Fig. 1. XRD pattern (a) and TCLP result of lead slag (b).

To be classified as non-hazardous waste, the leaching concentration of Pb should be lower than 5 mg/L, while there is no limit of Fe [15, 16]. The results obtained with the TCLP in Fig.1 showed that the original sample of lead slag was significantly higher than the standard. High leachability indicates greater potential harm to the environment. Although elements combined in lead slag are not contact with leaching solutions directly, there are potential mobility of heavy mobility and it should not be considered safe for environment if landfilled or processed for building materials.

3.2 Batch experiments

To optimize the efficiency of lead leaching in lead slag, the effect of operating parameters such as liquid/solid ratio, stirring rate, temperature, methanesulfonic acid concentration on recovery of lead was examined. The experiment of stirring rate was investigated in the range of 200 to 600 rpm. The determination of the mass transfer and diffusion is the key to influence the speed in the leaching process [17]. The stirring intensity play an important role in the reaction rate during the solid-liquid reaction, which increased the leaching rate by 40%–70% [18]. However, the stirring rate didn't influent leaching rate in Fig.3, which suggest the mass transfer is not affected by fluid film surrounding the solid particles, and the liquid film diffusion is not a control step of this process. The result of the effect of liquid-solid ratio between 5:1 and 40:1 was shown that the larger the liquid-solid ratio has a higher the leaching rate of lead. When the liquid-solid ratio is large, the viscosity and diffusion resistance of solutions could be reduced to improve the leaching rate [19]. The effect of methanesulfonic acid concentration ranging from 0.5 to 5 mol/L was studied. Fig.2 shows that the leaching efficiency is increasing with an increasing concentration, which indicate that the accelerate dissolution of lead slag.

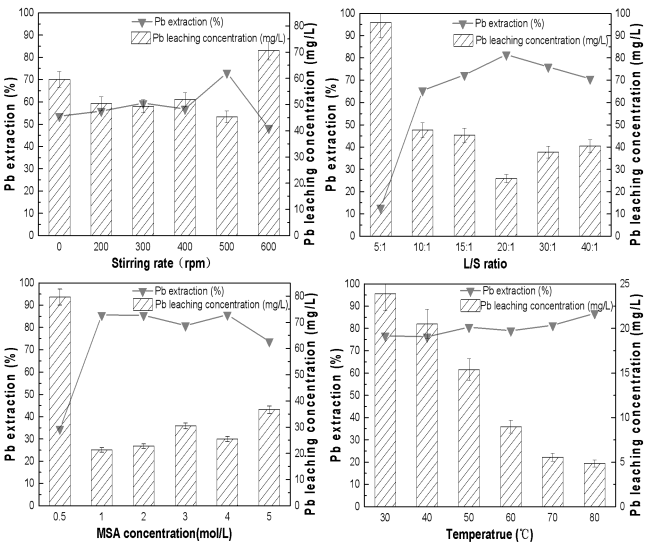

Fig. 2. Pb extraction and TCLP result of Pb leaching concentration of the residue at various string rates, L/S ratios, MSA concentrations and temperatures.

3.3 Kinetic analysis

After optimizing the parameters, then the kinetic study was performed in the optimized condition. The leaching results obtained at different temperature (40-80 °C) in Fig.3. The temperature influences the dissolution of lead, which has a significant effect on the complexation of methanesulfonic acid.

The application of shirking core models as Eq. (1), (2) and (3) was used to determine the lead leaching kinetics. In the leaching experiment, samples are taken regularly to analyse the leaching efficiency. Eq. (1) is a film diffusion-controlled process, while Eq. (2) is applicable to chemical reaction-controlled process. When the leaching reaction is in a diffusion-controlled process of stationary film, the kinetic reaction equation is according to Eq. (3), where α is the leaching efficiency of lead, k is the apparent chemical reaction rate, t is the leaching time.

$$\alpha = kt \tag{1}$$

$$1-(1-\alpha)^{\frac{1}{3}} = kt \tag{2}$$

$$1-\frac{2}{3}\alpha-(1-\alpha)^{\frac{2}{3}} = kt \tag{3}$$

Based on Eq. (1), (2), (3) and obtained data, α, $1-(1-\alpha)^{\frac{1}{3}}$, $1-\frac{2}{3}\alpha-(1-\alpha)^{\frac{2}{3}}$ value versus time were plotted in Fig.3. The experimental data was linearly fitted with a diffusion-controlled shrinking-particle model. It could be seen that Fig.3 showed a good linear relationship in the leaching experiment, indicating that the dynamic data of leaching reaction fitted the

diffusion-controlled shrinking-particle model well. The kinetic equation at each temperature was obtained from Fig.3 as Eq. (4), (5) and (6), where α is the leaching efficiency of lead, t is the leaching time.

$$40\ ℃: 1-\frac{2}{3}\alpha-(1-\alpha)^{\frac{2}{3}}=0.001145t-0.005101 \quad (4)$$

$$60\ ℃: 1-\frac{2}{3}\alpha-(1-\alpha)^{\frac{2}{3}}=0.001443t-0.003537 \quad (5)$$

$$80\ ℃: 1-\frac{2}{3}\alpha-(1-\alpha)^{\frac{2}{3}}=0.001606t-0.002197 \quad (6)$$

The correlation coefficients value corresponding to kinetic equations (4), (5) and (6) are 0.9753, 0.9694 and 0.9383 respectively, indicating that the measured data is in good agreement with the fitting equation.

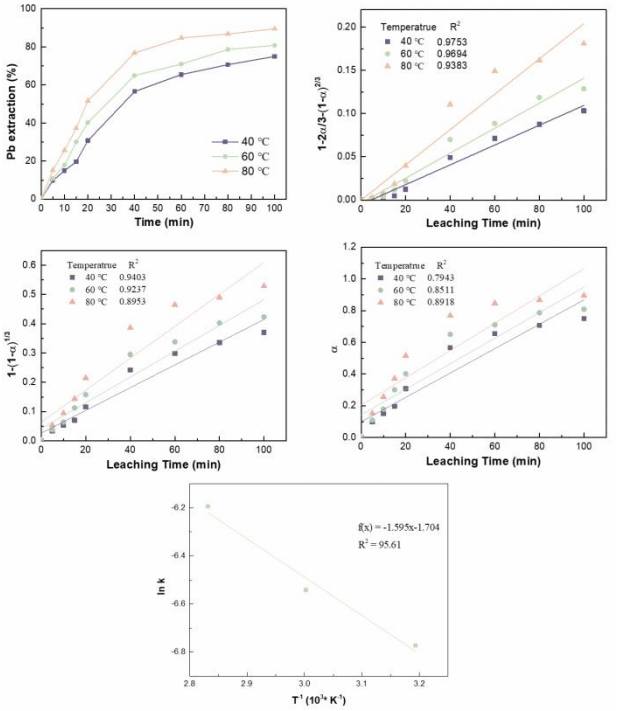

Fig. 3. Leaching rate of lead and linear relationship between 1-2α/3-(1-α)2/3 ,1- (1-α)1/3, α and leaching time in the leaching of lead slag at various temperatures, and Arrhenius plot of ln k vs. 1/T.

Considering the kinetic model of the diffusion-controlled process of stationary film, ln K values were plotted against 1/T according to Eq. (7), and the results, exhibit good linear relationships in Fig.3. The apparent activation energy for the leaching process can be obtained according to the Arrhenius law.

$$\ln K = -\frac{E}{RT}+B \quad (7)$$

The estimated apparent activation energy from the slope of fitted curve calculated as 13.621 kJ/mol according to Eq. (7) and Fig.3. The activation energy is within the range of internal diffusion control between 8 and 30 kJ/mol [20, 21], which further proves that the leaching reaction is a diffusion-controlled process of stationary film.

3.4 A proposed process for preparation of nano-structured PbO_2

In this study, a diaphragm electrodeposition device for fabricating PbO_2 was used to avoid the deposition of lead that made a cause of material loss and energy consumption caused on the anode in Fig.4. To realize the recycling of acid liquid, the anion exchange membrane was used to enrich the acid solution in the anode chamber, and the collected acid solution can be used in the leaching stage. The two products of electrolysis are separated and collected in two electrode chambers, which simplifies the operation and avoids product contamination.

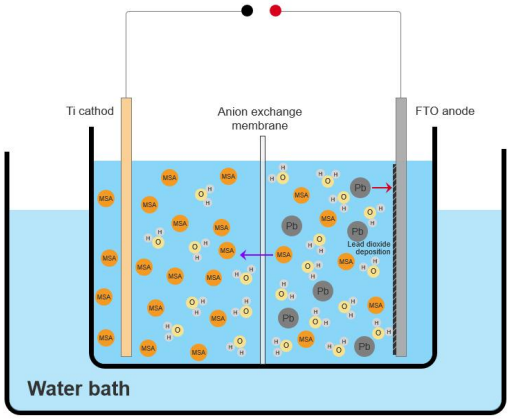

Fig. 4. Schematic of the diaphragm electrolysis cell.

Fig.5 shows the process of recovering and preparing nano-PbO_2 from waste lead slag. Lead slag is pre-treated as the above-mentioned leaching experiment, the solid sample was transformed into lead-containing methanesulfonic acid solution prepared for the next stage. Then PbO_2 was collected at the anode electrode by diaphragm electrolysis. The optimum temperature for calcining Pb_3O_4 was determined to be 400 °C, and the reaction time reached 10 h to obtain pure Pb_3O_4 from PbO_2. Pb_3O_4 obtained after calcination was added to acetic acid to obtain the precursor $Pb(CH_3COO)_4$. Pure nano-PbO_2 was obtained with the hydrolysis method as reported before. And the nanoparticles were range from 10-30 nm, which shows pure β-PbO_2 crystallization.

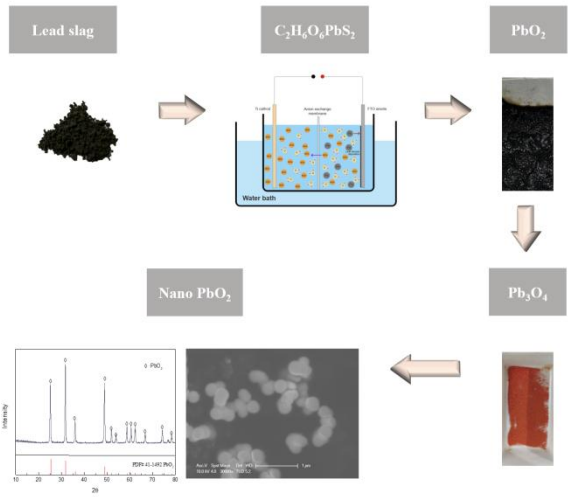

Fig. 5. Preparation of the nano-structured lead dioxide.

3.5 Application of nano-structured PbO_2

The obtained nano-PbO_2 was prepared according to the method as reported before [22] to prepare membrane electrode assembly for electrolyzing water to generate ozone, and its ozone-producing performance was measured as Fig.6.

Under the same current density, the cell voltage of obtained PbO_2 is basically the same as the cell voltage of nano-PbO_2 prepared with $Pb(CH_3COO)_4$ reagent. The output, current efficiency and energy consumption are also similar with the increase of current density. At 0.9 $A \cdot cm^{-2}$, the lowest energy consumption is about 182 wh $(gO_3)^{-1}$. The ozone-production of nano-PbO_2 recovered from waste lead slag and the nano-PbO_2 prepared by pure reagent is equivalent. Therefore, waste lead slag be employed to the preparation of nano-PbO_2 to realize the recycling of lead resources.

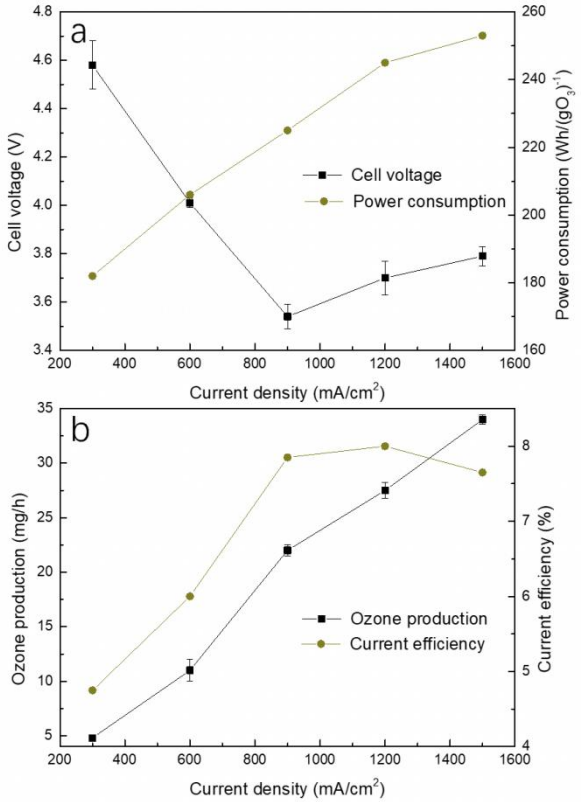

Fig. 6. The cell voltage and energy consumption (a), ozone production and current efficiency (b) with different current density.

4 Conclusion

In this research, the preparation and application of nano lead dioxide from lead slag is studied. In leaching system, the factor of stirring speed, temperature, methanesulfonic acid concentration, and liquid/solid ratio on the leaching performance of lead slag were investigated. The optimum condition of stirring rate 500 rpm, L/S ratio 20, 1 mol/L methanesulfonic acid, and 80 °C resulted in lead extraction of 89% and residue obtained without toxicity. The kinetics of leaching process was linearly fitted with a diffusion-controlled shrinking-particle model. Additionally, the Arrhenius diagram was plotted for leaching reaction and the apparent activation energy was obtained as 13.621 kJ/mol. Nano-PbO_2 recovered from waste lead paste was prepared for the electrolysis of water to produce ozone. The experimental results showed that the ozone production of nano-PbO_2 recovered from waste lead slag was not significantly different from the nano-PbO_2 prepared by pure reagents. In conclusion, waste lead slag can be employed to the fabrication of nano-PbO_2, which has a significant advantage on realizing the recycling of lead resources.

References

1. M. Alwaeli, Investigation of gamma radiation shielding and compressive strength properties of concrete containing scale and granulated lead-zinc slag wastes - ScienceDirect. Journal of Cleaner Production, **166**, 157-162 (2017)
2. F. Dai, et al., Recovery of high purity lead from spent lead paste via direct electrolysis and process evaluation. Separation and Purification Technology, **224**, 237-246 (2019)
3. J. Zhang, et al., A new pre-desulphurization process of damped lead battery paste with sodium carbonate based on a “surface update” concept. Hydrometallurgy, 2016. 160: p. 123-128.
4. A. Potysz, E.D. van Hullebusch and J. Kierczak, Perspectives regarding the use of metallurgical slags as secondary metal resources - A review of bioleaching approaches. Journal of Environment Management, **219**, 138-152 (2018)
5. C.S. Chen, Y.J. Shih and Y.H. Huang, Recovery of lead from smelting fly ash of waste lead-acid battery by leaching and electrowinning. Waste Management, **52**, 212-220 (2016)
6. J. Tang and B.M. Steenari, Leaching optimization of municipal solid waste incineration ash for resource recovery: A case study of Cu, Zn, Pb and Cd. Waste Management, **48(FEB.)**, 315-322 (2016)
7. F. Forte, et al., Closed-loop solvometallurgical process for recovery of lead from iron-rich secondary lead smelter residues. Rsc Advances, **7(79)** (2017)
8. E. Kim, et al., Process development for hydrometallurgical recovery of valuable metals from sulfide-rich residue generated in a secondary lead smelter. Hydrometallurgy, **169**, 589-598 (2017)
9. H. Wang, et al., Direct oxidative pressure leaching of bismuth sulfide concentrate in methanesulfonic acid medium. Hydrometallurgy, **194**, 105347 (2020)
10. T.J. O'brien, Method for measuring the quantity of lead on the surface of a brass component. US5612224 A (2017)
11. Z. Wu, et al., Fundamental study of lead recovery from cerussite concentrate with methanesulfonic acid (MSA). Hydrometallurgy, **142**, 23-35 (2014)
12. B.P. Chaplin, Critical review of electrochemical advanced oxidation processes for water treatment

applications. Environmental Science: Processes and Impacts, **16(6)**, 1182-1203 (2014)

13. T. Chen, et al., Electrochemical sensing of glucose by carbon cloth-supported Co3O4/PbO2 core-shell nanorod arrays. Biosens Bioelectron, **53**, 200-206 (2014)
14. S.C. Stark, et al., Assessment of metal contamination using X-ray fluorescence spectrometry and the toxicity characteristic leaching procedure (TCLP) during remediation of a waste disposal site in Antarctica. Journal of Environmental Monitoring, **10** (2010)
15. G.M.F. Gomes, T.F. Mendes and K. Wada, Reduction in toxicity and generation of slag in secondary lead process. Journal of Cleaner Production, **19(9-10)**, 1096-1103 (2011)
16. A. Smaniotto, et al., Qualitative lead extraction from recycled lead-acid batteries slag. Journal of Hazardous Materials, **172(2-3)**, 1677-80 (2009)
17. X. Deng, X., et al., Hydrothermal desulfurization of spent lead paste based on comproportionation reaction. Separation and Purification Technology, **259**, 118115 (2021)
18. X. Zhu, X. Liu, and Z. Zhao, Leaching kinetics of scheelite with sodium phytate. Hydrometallurgy, 186, 83-90 (2019)
19. W. Liu, et al., Preparation of calcium stannate from lead refining slag by alkaline leaching-purification-causticization process. Separation and Purification Technology, **212**, 119-125 (2019)
20. J.S.J.V. Deventer, Kinetics of metallurgical processes. Minerals Engineering, **13(3)**, 329-330 (2020)
21. G. Shi,et al., Kinetics of copper extraction from copper smelting slag by pressure oxidative leaching with sulfuric acid. Separation and Purification Technology, **241**, 116699 (2020)
22. X. Wu, Facile Synthesis of β-PbO2 Nanoparticles Range from 10–30 nm and their Application for Ozone Generation. Journal of The Electrochemical Society, **168(12)**, 123504 (9pp) (2021)